Fast cross-projection algorithm for reconstruction of seeds in prostate brachytherapy

Sreeram Narayanan[a)]
Department of Electrical Engineering, University of Washington, Seattle, Washington 98195-6043

Paul S. Cho[a)]
Department of Electrical Engineering, and Department of Radiation Oncology, University of Washington, Seattle, Washington 98195-6043

Robert J. Marks II
Department of Electrical Engineering, University of Washington, Seattle, Washington 98195-6043

(Received 19 November 2001; accepted for publication 3 May 2002; published 21 June 2002)

A fast method of seed matching and reconstruction in prostrate brachytherapy is proposed. Previous approaches have required all seeds to be matched with all other seeds in other projections. The *fast cross-projection algorithm for the reconstruction of seeds* (Fast-CARS) allows for matching of a given seed with a subset of seeds in other projections. This subset lies in a proximal region centered about the projection of a line, connecting the seed to its source, onto other projection planes. The proposed technique permits a significant reduction in computational overhead, as measured by the required number of matching tests. The number of multiplications and additions is also vastly reduced at no trade-off in accuracy. Because of its speed, Fast-CARS can be used in applications requiring real-time performance such as intraoperative dosimetry of prostate brachytherapy. Furthermore, the proposed method makes practical the use of a larger number of views as opposed to previous techniques limited to a maximum use of three views. [DOI: 10.1118/1.1489044]

Key words: seed reconstruction, prostate brachytherapy, intraoperative dosimetry

I. INTRODUCTION

Permanent implantation of radioactive seeds is a viable and effective therapeutic option widely used today for early-stage prostate cancer.[1] Although the implant procedure has improved in recent years with the help of computerized treatment planning and image guidance techniques, a significant enhancement of clinical outcome is expected from implementation of real-time intraoperative dosimetry and optimization. The intraoperative evaluation of dose delivery would permit the identification of underdosed regions and remedial seed placement, thus ensuring that the entire prostate volume receive the prescribed dose. However, before the concept can be realized, the problem of real-time seed localization must be solved. This is the motivation behind the present study, which addresses the speed of three-dimensional 3-D seed coordinate reconstruction. The related topic of automated determination of input, 2-D seed coordinates has been addressed elsewhere.[2,3]

Amols and Rosen[4] suggested an algorithm using a stereo pair and one anterior–posterior (AP) film. The reconstruction process involves dividing the implant into variable width bands of five to eight seeds each. These bands, formed by comparing y coordinates (Fig. 1) of films, cannot be relied upon due to the possible improper film placement and patient movement. Moreover, this method proves to be complicated and unreliable when the implant density is large. Biggs and Kelly[5] also used the y coordinate value as a screening mechanism to reduce the matching time. Their matching involves the process of selection and elimination. Due to potentially increasing ambiguities, this method diminishes in effectiveness as the seed count increases. Both methods, though moderately fast, can be used only for coplanar films.

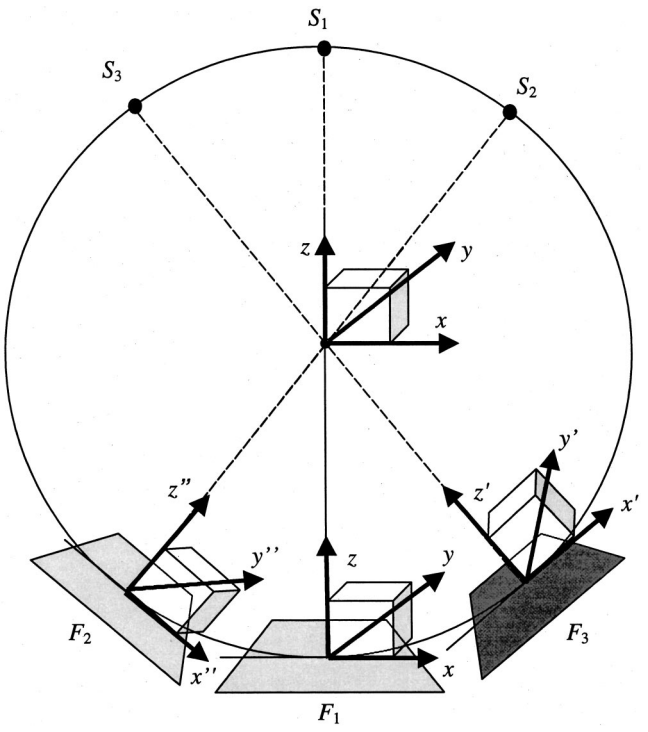

FIG. 1. The coordinate system.

Altschuler *et al.*[6] suggested an algorithm, which involves the use of fiducials for registration between the coordinates and correction of images. This may not be always practical as a fiducial object must be attached to the patient's skin. Jackson[7] proposed a method, which puts certain limitations on the geometry of images. The procedure imposes a constraint that the seeds implanted be regularly spaced in a line. Roy *et al.*[8] and Brinkman and Kline[9] proposed different methods using computed tomography (CT) for seed localization. These methods are limited by low resolution in the *z* direction due to interslice distance. The methods using CT can detect the centroid of the seeds only and assume that the seeds are parallel to the *y axis*. Also, CT will fail in resolving seeds connected end to end in the implant.

The Siddon and Chin[10] algorithm involves creating a cost function matrix of all possible seed combinations. Exhaustive matching using all possible combinations within the matrix is done to find the lowest cost solution. This method, while allowing a reasonably accurate match without any constraint on the film geometry, requires a large amount of computation for three films. Altschuler and Kassaee[11] suggested an innovative method of permutation sampling to reduce the matching complexity. This speeds up the matching process but still requires matching each seed on a projection with every seed on the other projections to calculate the cost function matrix.

The algorithm we propose, *fast cross-projection algorithm for the reconstruction of seeds* (Fast-CARS), is designed to further improve the computational efficiency. We cross-project the seeds between films (or views) pairwise to form linear, variable-width bands on all the views. Each band contains a fraction of the total number of seeds. With this process, matching of a relatively small number of seeds among all the bands is assured. The process can be repeated to cover all seeds in every view. After a set of search restriction bands is formed, the cost function proposed by Siddon and Chin is used to form a matrix of costs. Alternately, for noncoplanar x-ray source trajectory, the cost functions proposed by Altschuler and Kassaee[11] can be employed. For each cost matrix an exhaustive match can be performed to obtain the best possible matches. Let the number of seeds be N. If the average number of seeds in a band is A and the number of such bands is K, then the process requires $K\times(A!)^2$ matches. Since $A \ll N$, this is a great reduction when compared to $(N!)^2$ comparisons, as proposed by Siddon and Chin. To illustrate, if there are $N=64$ seeds and, on average, eight seeds in a band ($A=8$), then with eight such bands ($K=8$) the Fast-CARS requires 1.3×10^{10} comparisons, a great reduction from $1.6\times10^{178}=(64!)^2$ as required without the use of the bands. There is also a correspondingly significant reduction in the number of multiplications and additions. We need not calculate a huge cost function matrix involving all possible seed combinations over all the views. Rather, calculation is performed only on a subset of seeds confined within each band.

In Sec. II we discuss the properties of two noteworthy methods previously published.[10,11] Section III contains a presentation of the details of Fast-CARS. The experimental setup and simulations are explained in Sec. IV. In Sec. V, we provide simulation results and a discussion.

II. SEED RECONSTRUCTION ALGORITHMS: PREVIOUS WORKS

A method for the 3-D reconstruction of seeds, commonly used in clinical practice, was proposed by Siddon and Chin.[10] Each seed is back-projected to the source for three seed images on three different radiographs. The shortest distance from the point of closest approach to each of the rays is calculated. The resulting root-mean-square (rms) sum for each chosen triplet forms an entry in the cost function matrix. In the absence of uncertainty due, for example, to noise or patient movement, the three back-projected rays will intersect at one point if they belong to the image of the same seed in the three radiographs. The value corresponding to this seed triplet in the cost-function matrix is zero and the point of intersection of the three rays is the true 3-D location of the seed.

To find the best seed triplet set, choose N elements from the cost function matrix such that no seed image in a radiograph is counted twice. Here, for simplicity of presentation, assume all N seeds are visible on each radiograph. We calculate the sum of these N elements and repeat the process for all possible choices of N elements using the above constraint. The combination of seeds, which gives the lowest error sum, is considered the best triplet set. The point of closest approach for each triplet of seed images is considered the 3-D seed coordinate.

Altschuler and Kassaee[11] proposed an alternate method for matching. After creating a cost function matrix using three views, a random seed image is chosen and the best possible match of that seed image in the other two radiographs is identified. This process is repeated, taking into consideration that no seed image is used twice. Repeated application results in the matching of all seeds. The matching of all seeds is repeated a number of times using a different starting radiograph and a different ordering of seeds. After numerous applications, the seed matching with the lowest rms error is chosen.

These approaches do not make use of the information regarding seed position on the radiographs. For example, in coplanar images, for proper film placement, we know the seed image in the upper portion of one radiograph will not match an image located at the bottom part of another radiograph. Thus, calculating cost functions for such unrelated image components is computationally inefficient. A more efficient approach is to make use of some geometrical and positional information to match a given seed with other seeds. This paper proposes a procedure to do so. Unlike previous approaches,[4,5] Fast-CARS does not require that the films be stereo pairs, orthogonal, or even coplanar. Fast-CARS can be applied without any *y* coordinate matches and correction.[12] The bands of seeds are not formed by looking at the films and the positional coordinates, but, rather, by cross-projecting the line connecting seed images and their corresponding point radiation source.

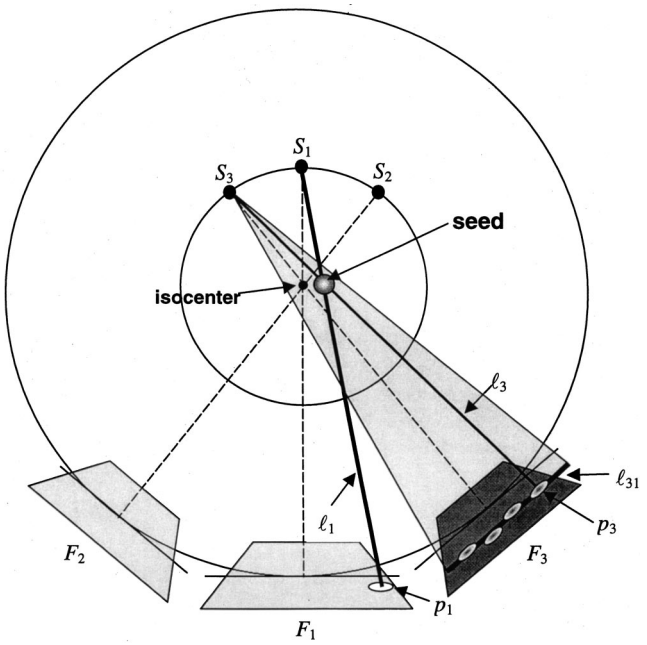

FIG. 2. Obtaining the projection of the line connecting a seed image and source on another film. A seed image is chosen at random from F_1 and back-projected to S_1. The projection of this line is formed on F_3. The dotted lines show the projection of the 3-D point, the point of intersection of the line, and the plane. The dark line connecting the end points of the two projections is the 2-D projection of the line F_1-S_1.

III. ALGORITHM

The coordinate system proposed by Siddon[13] is used throughout this paper (Fig. 1). Consider, as illustrated in Fig. 2, three radiographs, each recording N seed images. Shown in the middle of the figure is an example seed in space, projected onto three film planes F_1, F_2, and F_3 from three x-ray source positions S_1, S_2, and S_3. The inner circle represents the locus of locations of the radiation source and the outer circle the locus of the film-plane points closest to the x-ray source. In a noiseless case, a line connecting the seed image and the corresponding source will pass through the actual 3-D position of the seed. For example, the line connecting the known projection point, P_1, and the x-ray source, S_1, must pass through the unknown seed coordinates. The line is labeled as l_1. A 2-D projection of l_1 onto F_3 results in a line on which the seed projection must lie. For example, the projection of l_1 onto film plane F_3 is the line l_{31}. The projection, P_3, of the unknown seed coordinates onto F_3, independent of the seed location on line l_1, must lie at some point on the line l_{31}. Therefore, in searching for the seed projection on F_3 that matches the projection P_1, attention can be limited to line l_{31} rather than the entire F_3 plane. This is the essence of Fast-CARS.

In the presence of small uncertainties, such as incremental patient movement and digitization error, the line l_{31} will pass close to, rather than directly through, the actual seed image. The band, B_{31}, centered on line l_{31}, will contain only a few ambiguous seeds that cast doubt on the true identity of the cross-projected seed. We can limit the matching of the seed image to those included in the band.

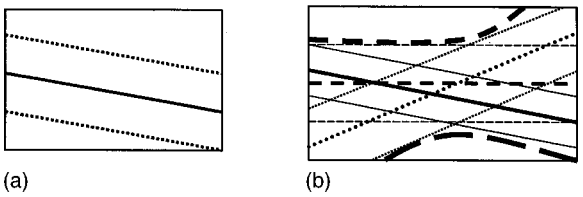

FIG. 3. (a) Shown above is the band on one film, where only the projection of a single seed image-source line is taken (solid line). The dotted lines are the edges of the band corresponding to this line. (b) Here the projection of all the seeds from the band on the left is shown. As we can see, there are three darker lines corresponding to the projection of the seed-image–source lines. The lighter lines on either side are its bands. All the seeds lying in the union of the bands (between two dark curves) are taken for matching.

Let us call the bands formed in the three radiographs B_1, B_2, and B_3, respectively. Our algorithm involves the following steps.

(1) Select a seed image from F_1.
(2) Obtain the projection of the line connecting the seed image and S_1 on F_2.
(3) Form a search restriction band, B_2, on F_2 centered on the projected line.
(4) Take a seed image from B_2 and connect it to source S_2.
(5) Obtain the projection of this line on F_1 and F_3.
(6) Generate bands centered around these lines on F_1 and F_3.
(7) Repeat steps (4)–(6) over all seed images of B_2.
(8) Form B_1 and B_3, a union of all the bands, in F_1 and F_3, respectively.
(9) Match all seeds in B_1, B_2, and B_3.
(10) Repeat steps (1)–(9) using an unmatched seed in F_1 until all seeds have been matched.

A. Generation of search restriction bands

A line connecting the 2-D seed image and its corresponding source will pass through the actual 3-D location of the seed. The projection of a segment of this line can be formed on films taken at other angles. Using the same labels as above we will show how the projections of these lines are obtained.

Any two points on the film plane, F_2, and the corresponding x-ray source position, S_2, will constitute three unique points that can define a plane. The line connecting the seed image on another film, F_1, and its source, S_1, will intersect this plane at a point. Projection of this point onto the 2D film plane, F_2, can be obtained. It will be referred to as P_1. Similarly, two other points on the same plane, F_2, and source, S_2, define another plane, whose point of intersection with the same line can be found. The projection of this point of intersection will yield a point on F_2. It will be referred to as P_2. The line L joining P_1 and P_2 is identified to a projection of l_1, the line connecting the seed image on F_1 to S_1, onto F_2. As a convention we use two adjacent corner points on the film plane as the first two points, and its corresponding opposite corners as the other two points to form the planes. The equations for calculating the above can be found in the Appendix. Now let the equation of the line, L, be y_L

TABLE I. A comparison of timings in seconds between the two algorithms for three and four views. Calculations were performed on a 600 MHz computer. The sizes of the bands were kept at 1.2 cm for all experiments.

	Three views		Four views	
Number of seeds	Without-CARS (s)	Fast-CARS (s)	Without-CARS (s)	Fast-CARS (s)
60	6	1	340	18
90	20	4	1233	56
120	47	8	5505	342
150	91	33	13599	867
200	216	80	42525	3637

$=mx_L+b$, where b is the Y intercept. If $2k$ is the width of the band, let $b^- = b-k$ and $b^+ = b+k$. If the Y coordinate of the seed image satisfies the following relationship, $mx+b^- < y < mx+b^+$, then the seed belongs to the band centered on L, where x and y are the two-dimensional coordinates of the seed image. When several bands are on one film, the union of all the seeds from each of the bands may be formed as shown in Fig. 3, which can then be used for subsequent matching and the reconstruction process.

B. Seed matching and reconstruction

The method proposed by Siddon and Chin[10] is used to calculate the 3-D location of the seed and the cost function matrix for the reconstruction. The seeds used for back-projection here are the ones in B_1, B_2, and B_3. In such a case the cost function matrix will be very small. Since we have discarded the uncorrelated triplets, there is a reduction in the number of times a possible seed position is calculated as compared to previous methods. We can then perform either an exhaustive combinatorial optimization[10] or do the permutation sampling[11] to get the best triplets. In our work the latter method was used for improved efficiency. Since we already know the assumed end coordinates from calculating the cost function matrix, the 3-D end points can be extracted quickly and used for the dose calculation. In summary, our algorithm consists of the following steps.

(1) Perform cross-projection to form search limiting bands on images.
(2) Calculate the cost-function matrix for the seeds within the individual bands alone, using the Siddon–Chin method.
(3) Perform permutation sampling on the cost-function matrix obtained in step #2 to determine the best triplet set.

IV. ALGORITHM TESTING

A. Simulation studies

Simulation studies were performed using computer-generated data. The algorithms were coded in C++ in Windows 2000 environment and simulations performed on a 600 MHz PC. The length of the seed was taken to be 0.3 cm. For our setup the source-to-isocenter distance was 100 cm and the source-to-film distance was 140 cm. The seeds were randomly generated within a 5 cm cube centered about the isocenter. For the three-view technique the images were simulated at gantry angles of 0°, 15°, and −15°. For the fourth view, a −30° projection was added. The x-ray source was assumed to be a point source.

To test the algorithm performance, simulations were performed for various numbers of seeds in a noiseless environment. Subsequently, a slight translation in 3-D coordinates was introduced to simulate patient motion. Since patient motion can be assumed to be uniform over all the seeds, it can

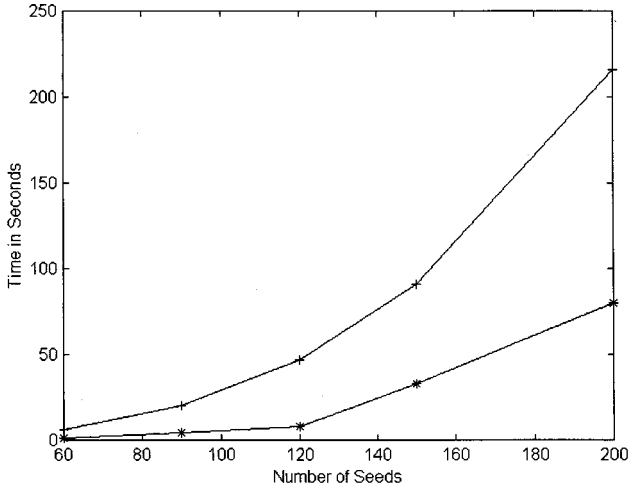

FIG. 4. A comparison of computational speed: 3-D seed reconstruction from three views. (+) Without-CARS; (*) Fast-CARS.

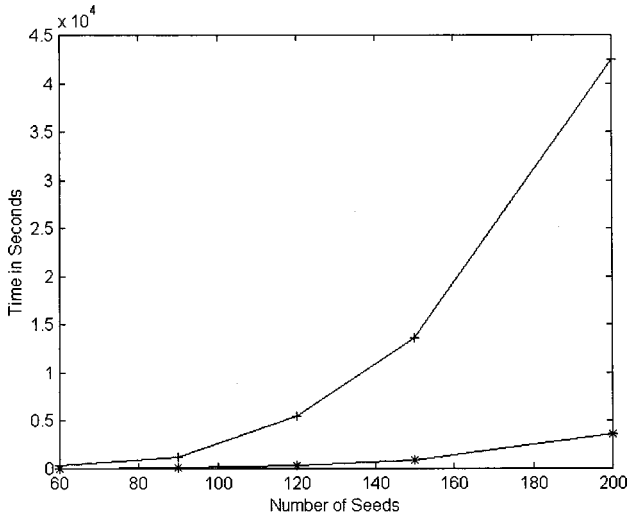

FIG. 5. A comparison of computational speed: 3-D seed reconstruction from four views. (+) Without-CARS; (*) Fast-CARS

TABLE II. (a) A three-view example: a comparison of mismatches in the presence of translation errors, E_1. E_1 is a uniform shift of all seeds in the x and y direction. N is the number of seeds. Three views were equally spaced at 15-degree increments. The width of the search restriction band was chosen to compensate for the amount of translation in the system. (b) A three-view example: comparison of mismatches in the presence of segmentation/digitization error, E_2. E_2 is the standard deviation of a random Gaussian noise added around the 2-D seed coordinates. Bands of size 1.2 cm were used.

(a)

E_1 (cm)	$N=20$	$N=40$	$N=60$	$N=80$	$N=100$	$N=120$	Band size (cm)
0.0	0	0	0	0	0	0	1.2
0.2	0	0	0	0	0	0	1.2
0.4	0	0	0	0	0	0	1.6
0.6	0	0	0	0	0	0	1.8
0.8	0	0	2	4	4	6	2.0
1.0	0	0	4	4	6	8	2.0

(b)

E_2 (cm)	$N=20$	$N=40$	$N=60$	$N=80$	$N=100$	$N=120$
0.00	0	0	0	0	0	0
0.02	0	0	0	0	0	0
0.04	0	0	0	0	0	0
0.06	0	0	0	0	0	0
0.08	0	0	0	0	2	4
0.10	0	0	2	2	2	4

be simulated by translation in the x and y directions. This can be done by adding a constant vector, E_1, to the 3-D coordinates of the seeds. The amount of translation was varied from 0.2 to 1.0 cm and the mismatches were noted in each case. In addition, Gaussian noise, E_2, was added around the seed end coordinates to simulate digitization/segmentation errors. Since the errors in consideration are usually on the order of a few pixels, the noise added was kept to zero mean Gaussian with a standard deviation varying from 0.02 to 0.1 cm.

The width of the search restriction band was varied from 1.0 to 2.0 cm. The number of missed seeds (seeds not falling in their corresponding bands) and mismatches were noted. Too small a band will lead to seeds being missed and, hence, a mismatch during reconstruction. This is because the noise is so large that the seeds have migrated from their supposed position and will not fall in their corresponding band. This can occur in cases of a large amount of patient motion. Too wide a band is also not advisable since the number of seeds in each band will be large and will lead to unnecessary matching and reconstruction. Later, Table IV shows the effect of a search restriction bandwidth on matching accuracy for three views with 100 seeds each and 0.4 cm translation error in the y direction. We chose the y direction, as the

TABLE III. (a) A four-view example: comparison of mismatches in the presence of translation errors, E_1. Four views were equally spaced at 15-degree increments. Note the reduction in number of mismatches compared to the three-view example, Table 2a. (b) A four-view example: a comparison of mismatches in the presence of segmentation/digitization error, E_2. Again, the reduction in the number of mismatches compared to the three-view example, Table II(b), is noted. Bands of size 1.2 (cm) were used.

(a)

E_1 (cm)	$N=20$	$N=40$	$N=60$	$N=80$	$N=100$	$N=120$	Band size (cm)
0.0	0	0	0	0	0	0	1.2
0.2	0	0	0	0	0	0	1.2
0.4	0	0	0	0	0	0	1.6
0.6	0	0	0	0	0	0	1.8
0.8	0	0	0	0	3	4	2.0
1.0	0	0	0	3	4	4	2.0

(b)

E_2 (cm)	$N=20$	$N=40$	$N=60$	$N=80$	$N=100$	$N=120$
0.00	0	0	0	0	0	0
0.02	0	0	0	0	0	0
0.04	0	0	0	0	0	0
0.06	0	0	0	0	0	0
0.08	0	0	0	0	0	2
0.1	0	0	0	0	2	2

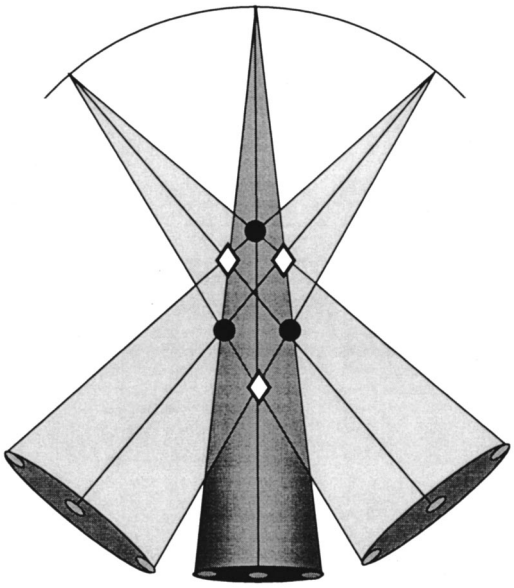

FIG. 6. The figure shows probable mismatches using three films. The rays shown are the back-projected rays from three seed images on three films to their respective sources. In this particular case there exist two ambiguous solution sets, denoted by the circles and the diamonds. The ambiguities can be resolved with an additional film.

bands are more susceptible to errors in this direction. A translation in x will cause the seeds to move in a direction parallel to the bands and therefore will not be a factor for the errors.

B. Phantom studies

In order to test the accuracy of Fast-CARS under the clinical setting, a test phantom was constructed. The phantom consisted of 20 dummy I-125 seeds (Standard Imaging, Middleton, WI) embedded in Lucite plates with known end point coordinates. The phantom was imaged with an image intensifier (Elekta SLS-14 simulator, Crawley, UK) using a 9 in. mode at gantry angles of 165°, 180°, and 195°. The acquired images were corrected for geometric distortion at subpixel accuracy.[14] Subsequently, the 2-D end coordinates of the seeds were determined using a seed localizer program.[2,3] The pixel resolution was 487 μm. The seed coordinates were then input to Fast-CARS for 3-D seed reconstruction.

TABLE IV. Effect of the search restriction bandwidth on matching accuracy and computational speed. The simulations were performed for 100 seeds with 0.4 cm translation error in the y direction.

Width of band (cm)	Number of mismatches	Execution time (s)
0.6	13	4
0.8	13	4
1.0	9	5
1.2	5	5
1.4	2	5
1.6	0	6
1.8	0	6
2.0	0	7

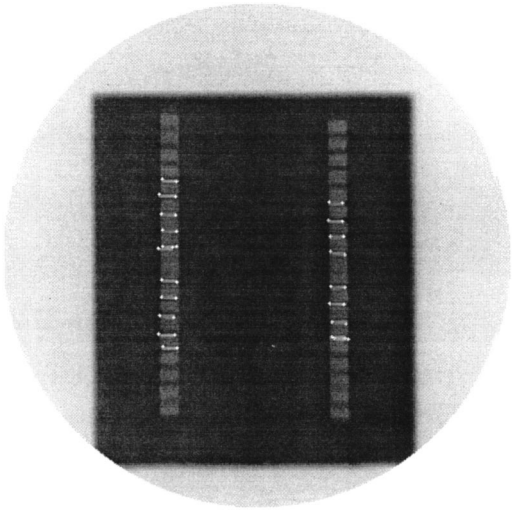

FIG. 7. In order to visualize the accuracy of the algorithm, the reconstructed 3-D seed end-point coordinates were forward projected onto the distortion-corrected fluoroscopy images. The example shown here is for the 180-degree gantry position. The seeds appear as light-gray segments and the white spots mark the end coordinates.

V. RESULTS AND DISCUSSIONS

A. Simulation studies

Table I and Fig. 4 show a comparison of the timings. The Fast-CARS consists of three components: (1) cross-projection from the search limiting bands in images, (2) the formation of cost function matrices according to Ref. 10, and (3) permutation sampling on the cost matrix based on Ref. 11 to determine the best triplet set. In order to assess the gain in computational speed due to a cross-projection algorithm, simulation studies were repeated without the benefit of component #1. Thus we compared Fast-CARS against a method with just two components, in which a matrix of cost functions with the full dataset was formed and the permutation sampling applied on the whole 3-D ensemble. This method will henceforth be referred to as "Without-CARS." The results indicate that for a typical range in number of seeds used in clinical practice, Fast-CARS is at least an order of magnitude faster than Without-CARS. Improvement in speed becomes even more remarkable when a comparison is made for reconstruction using four views (Table I and Fig. 5). The reconstruction speed will improve further as the computer processor speed continues to rise. Thus, the Fast-CARS makes the concept of real-time intraoperative dosimetry feasible and also the use of a large number of views clinically practical.

The efficacy of using a greater number of views is demonstrated empirically in Tables II and III. The results indicate that the occurrence of mismatches diminishes with the increase in the number of views. This can be understood in terms of cost function. For example, in order for a mismatch to occur in the four-view case, it would require all four components of the cost function to be large, which is less probable than the three-view situation, where only three components need to be erroneous. Use of an increased number of

views also helps resolve potential ambiguities in the matching process. It is well known that ambiguity in seed identification can exist with the two-view technique. It should be noted, however, that even with three views such ambiguities could occur. For example, in Fig. 6, we show the back-projected rays from three seed images on three views to their respective sources. For these three seeds there are two perfectly good solutions denoted by a set of diamonds and circles, of which only one is the correct solution, the other being a mismatch. This ambiguity can be resolved by adding a fourth view that is sufficiently spaced from the rest. In general, the possibility of ambiguous seed identity diminishes with the number of views.

Table IV shows the effect of the search restriction bandwidth on matching accuracy and speed. As shown in this example using 100 seeds and three views, for a translation error of 0.4 cm use of a narrow band led to large errors, even though the computation speed was fast. A more accurate reconstruction can be achieved at a small trade-off in execution time by increasing the bandwidth. For prostate brachytherapy in which the patient is kept under anesthesia, error due to patient motion is expected to be minimal.

B. Phantom studies

The reconstructed end-point coordinates were compared to the known values. The mean error and standard deviation in the x and the y direction were $410 \pm 615\ \mu$m and $218 \pm 293\ \mu$m, demonstrating the geometric fidelity of the entire image processing, including distortion correction and seed reconstruction process. Furthermore, in order to visualize the algorithm performance, the reconstructed coordinates were projected onto the distortion-corrected fluoroscopy images. As shown in Fig. 7, the agreement is excellent.

VI. CONCLUSIONS

The proposed cross-projection algorithm is a fast and accurate method for solving the seed reconstruction problem. The major advantage in speed comes from the savings in time in calculating a matrix of costs. Fast-CARS essentially reduces the search space by removing uncorrelated triplets. The algorithm can be applied to a large number of seeds for three or even four projections with near real-time performance. As such, it lends itself to time-constrained applications such as intraoperative dosimetry of prostate brachytherapy.

ACKNOWLEDGMENT

This work was supported in part by a grant from the National Institutes of Health, CA89061.

APPENDIX: PROJECTION OF LINE CONNECTING SEED IMAGE AND SOURCE ONTO A PLANE

Given a plane defined by three points P_1, P_2, P_3 and a line defined by two points L_1 and L_2, the point of intersection between the plane and the line can be determined as follows. Let the coordinates of the plane- and the line-defining points be

$$P_1=[x_1,y_1,z_1], \quad P_2=[x_2,y_2,z_2],$$

$$P_3=[x_3,y_3,z_3], \quad L_1=[x_4,y_4,z_4],$$

and

$$L_2=[x_5,y_5,z_5].$$

It is convenient to form matrices

$$A=\begin{bmatrix} 1 & 1 & 1 & 1 \\ x_1 & x_2 & x_3 & x_4 \\ y_1 & y_2 & y_3 & y_4 \\ z_1 & z_2 & z_3 & z_4 \end{bmatrix} \text{ and } B=\begin{bmatrix} 1 & 1 & 1 & 0 \\ x_1 & x_2 & x_3 & x_5-x_4 \\ y_1 & y_2 & y_3 & y_5-y_4 \\ z_1 & z_2 & z_3 & z_5-z_4 \end{bmatrix}.$$

Then the 3-D coordinates of the point of intersection, $(\hat{x}, \hat{y}, \hat{z})$, are given by

$$\hat{x}=x_4+t(x_4-x_5), \quad \hat{y}=y_4+t(y_4-y_5),$$

$$\text{and } \hat{z}=z_4+t(z_4-z_5), \quad \text{where} \quad t=\frac{|A|}{|B|}.$$

By convention, P_1 and P_2 are two points on a film plane, which we call F_1. The point P_3 corresponds to the source position associated with film F_1. L_1 represents the source position associated with film F_2. And L_2 is the coordinate of a given seed on film F_2 that is cross-projected onto F_1.

The projection of $(\hat{x}, \hat{y}, \hat{z})$ can be obtained on any film plane as follows:

$$u'=\frac{(\hat{x}-x_3)}{(\hat{z}-z_3)}\cdot d+x_3,$$

$$v'=\frac{(\hat{y}-y_3)}{(\hat{z}-z_3)}\cdot d+y_3,$$

where u' and v' are the projected coordinates of the 3-D point and d is the source to film distance. Given two such points on a film plane, a line can be formed. If the seed coordinates satisfy the conditions explained in Sec. III A, then it belongs to the band.

[a]Correspondence to Department of Radiation Oncology, University of Washington, Box 356043, Seattle, Washington 98195-6043. Telephone: (206) 598-4754; Fax: (206) 598-6218; electronic mail: psncho@u.washington.edu

[1] P. D. Grimm, J. C. Blasko, J. E. Sylvester, R. M. Meier, and W. Cavanagh, "10-year biochemical (prostate-specific antigen) control of prostate cancer with (125) I brachytherapy," Int. J. Radiat. Oncol., Biol., Phys. **51**, 31–40 (2001).

[2] P. Cho and B. Adams, "Automated seed recognition for intraoperative prostate brachytherapy dosimetry," Med. Phys. **26**, 1146 (abstract) (1999).

[3] P. S. Cho, "Computerized segmentation of clustered seeds in prostate brachytherapy," in *Proceedings of the 13th International Conference on*

the Use of Computers in Radiation Therapy, edited by W. Schlegel and T. Bortfeld (Springer-Verlag, Heidelberg, 2000), pp. 105–107.
[4] H. I. Amols and I. I. Rosen, ''A three-film technique for reconstruction radioactive seed implants,'' Med. Phys. **8**, 210–214 (1981).
[5] P. J. Biggs and D. M. Kelly, ''Geometric reconstruction of seed implants using a three-film technique,'' Med. Phys. **10**, 701–704 (1983).
[6] M. D. Altschuler, P. A. Findlay, and R. D. Epperson, ''Rapid, accurate, three-dimensional location of multiple seeds in implant radiotherapy treatment planning,'' Phys. Med. Biol. **28**, 1305–1318 (1983).
[7] D. D. Jackson, ''An automatic method for localizing radioactive seeds in implant dosimetry,'' Med. Phys. **10**, 370–372 (1983).
[8] J. N. Roy, K. E. Wallner, P. J. Harrington, C. C. Ling, and L. L. Anderson, ''A CT-based evaluation method for permanent implants: Application to Prostate,'' Int. J. Radiat. Oncol., Biol., Phys. **26**, 163–169 (1993).
[9] D. H. Brinkmann and R. W. Kline, ''Automated seed localization from CT datasets of the prostate,'' Med. Phys. **25**, 1667–1672 (1998).
[10] R. L. Siddon and L. M. Chin, ''Two-film brachytherapy reconstruction algorithm,'' Med. Phys. **12**, 77–83 (1985).
[11] M. D. Altschuler and A. Kassaee, ''Automated matching of corresponding seed images of three simulator radiographs to allow 3D triangulation of implanted seeds,'' Phys. Med. Biol. **42**, 293–302 (1997).
[12] M. S. Rosenthal and R. Nath, ''An automatic seed identification technique for interstitial implants using three isocentric radiographs,'' Med. Phys. **10**, 475–479 (1983).
[13] R. L. Siddon, ''Solution to treatment planning problems using coordinate transformations,'' Med. Phys. **8**, 766–774 (1981).
[14] P. S. Cho, R. H. Johnson and T. W. Griffin, ''Cone-beam CT for radiotherapy applications,'' Phys. Med. Biol. **40**, 1863–1883 (1995).